

## Supporting information

### Unusual Chirality Transfer from Silica to Metallic Nanoparticles with Formation of Distorted Atomic Array in Crystal Lattice Structure

Seiji Tsunega,<sup>1</sup> Toyokazu Tanabe,<sup>2</sup> and Ren-Hua Jin<sup>1\*</sup>

<sup>1</sup>Department of Material and Life Chemistry, Kanagawa University, 3-2-7 Rokkakubashi,  
Yokohama 221-8686, Japan

<sup>2</sup>Department of Materials Science and Engineering, National Defense Academy, 1-10-20  
Hashirimizu, Yokosuka 239-8686, Japan  
E-mail: Ren-Hua Jin - [rhjin@kanagwa-u.ac.jp](mailto:rhjin@kanagwa-u.ac.jp)

### Additional description for Scheme 1

As shown in Scheme 1, the preparation of Ag and Au NPs in chiral silica is slightly different in the step of insertion metal ions into silica. Usually, silica is not easy to adsorb cationic substances both of metallic and organic ones due to positive charge feature of silanol Si-OH. This feature should be taken into account in advance when we perform the chiral transfer from silica to metallic NPs.  $\text{Ag}^+$  is cation (when using  $\text{AgOAc}$ ), so we need to locate anion inside of silica to accept  $\text{Ag}^+$ . Just tartrate anions are presence in the chiral silica bundles of PEI/Tart/ $\text{SiO}_2$ , they can trap effectively  $\text{Ag}^+$  ions. In case of using  $\text{HAuCl}_4$ , however, the  $[\text{AuCl}_4]^-$  is anion, so the anionic Tart should be removed from silica while retaining basic PEI inside. Otherwise, we could not effectively concentrate metallic substances into silica.

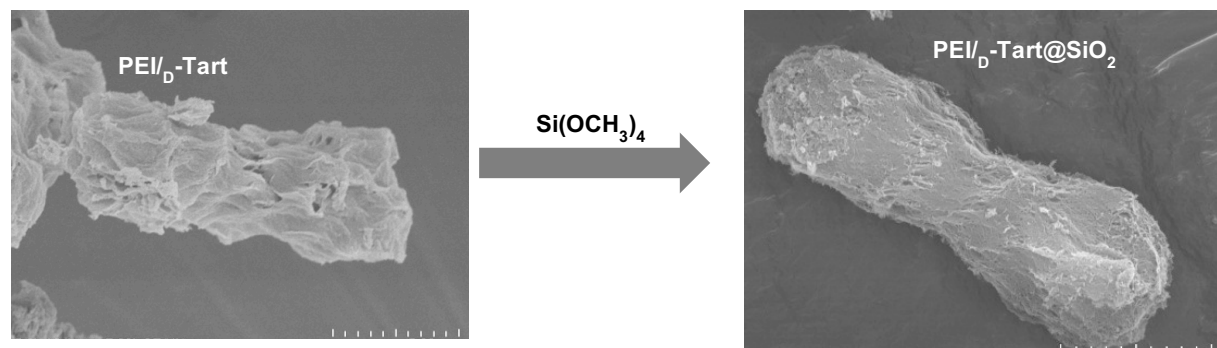


**Fig. S1.** SEM images of the boundles of PEI/<sub>D</sub>-Tart complexe and its corresponding product of PEI/<sub>D</sub>-Tart@ $\text{SiO}_2$ . Scale bars: 5 mcirometer.

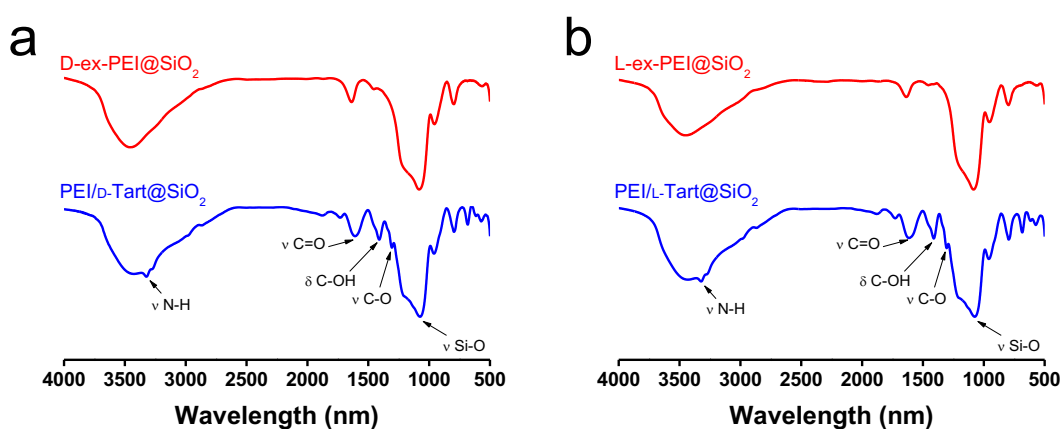


**Fig. S2.** FT-IR spectra of a) D-form and b) L-form samples (blue line for PEI/Tart@ $\text{SiO}_2$ , red line for ex-PEI@ $\text{SiO}_2$ ).

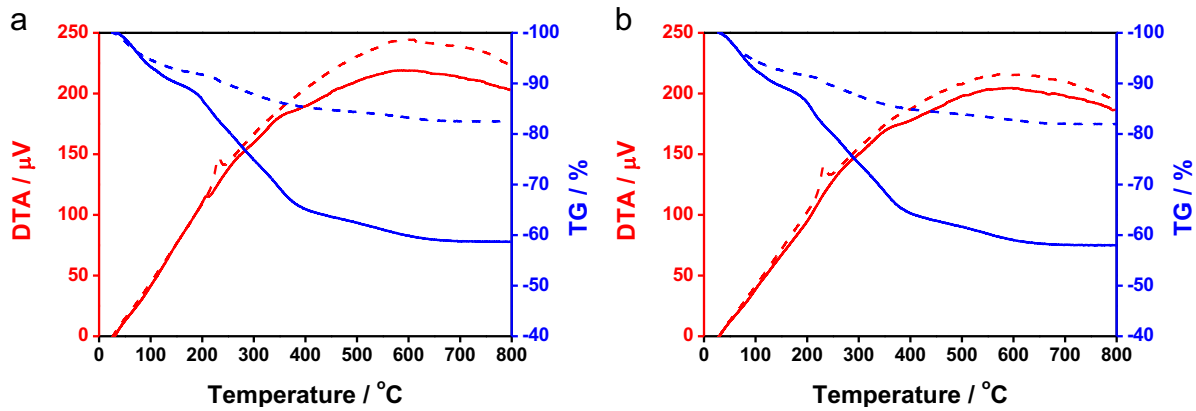


**Fig. S3.** The TG and DTA curves for a) D-PEI/tart@SiO<sub>2</sub> (solid) and D-ex-PEI@SiO<sub>2</sub> (dot), and b) L-PEI/Tart@SiO<sub>2</sub> (solid) and L-ex-PEI@SiO<sub>2</sub>(dot) (blue lines for TG, red lines for DTA). It is obvious that the weight-loss became smaller nearly by 20% for both case of D- and L-forms after washing the as-prepared hybrids of PEI/Tart@SiO<sub>2</sub> by NH<sub>4</sub>OH (aq). This means that the remove of tartrate component from the hybrids is very efficient.

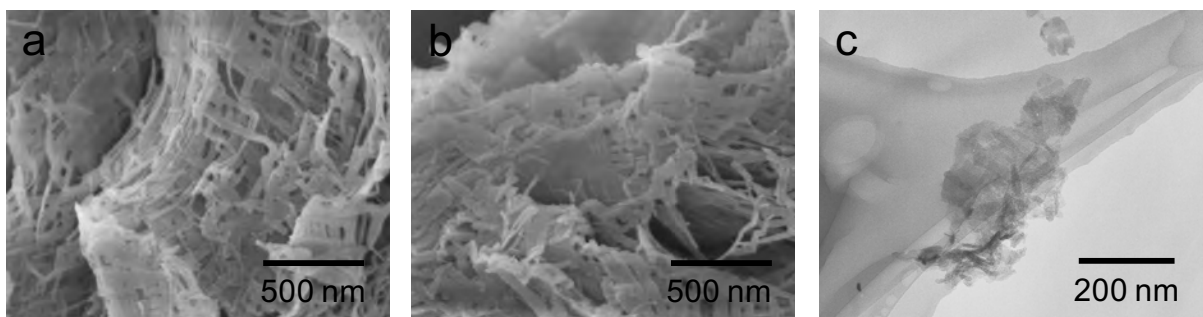


**Fig. S4.** SEM images of the as-prepared hybrids bundles of PEI/D-Tart@SiO<sub>2</sub> (a) and PEI/L-Tart@SiO<sub>2</sub> (b). TEM image of the piece of D-SiO<sub>2</sub> (c) crushed by homogenizing the methanol solution containing chiral silica bundles (obtained from calcination of PEI/Tart@SiO<sub>2</sub> at 600 °C) with the proviso that is 20,000 rpm for 2 min.

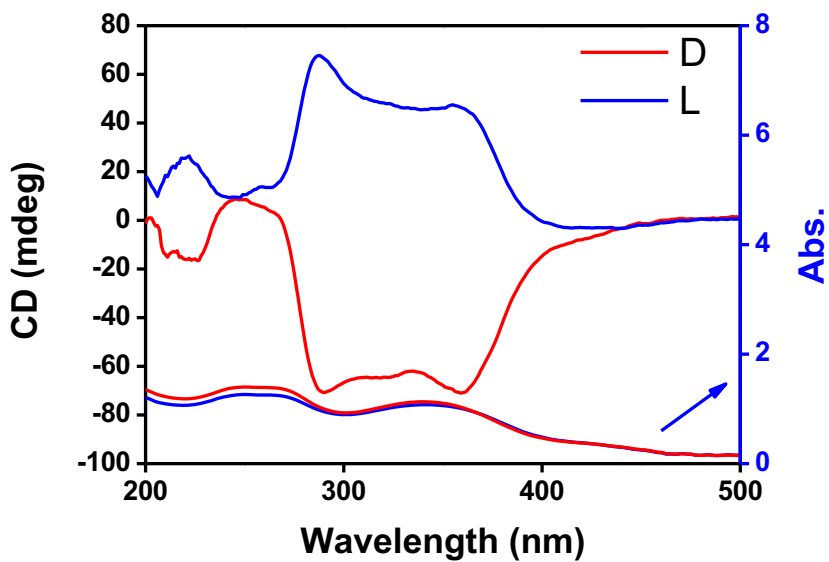


**Fig. S5.** DRCD and UV-Vis spectra of the calcined PEI/tart@ $\text{SiO}_2$  combined with 2-methyl-1,4-naphthoquinone (MNQ) (blue lines for L- $\text{SiO}_2$ , red lines for D- $\text{SiO}_2$ ). The chiral silica samples calcined at 600°C were mixed with 10 wt% MNQ in KCl and used for measurement of DRCD. Obviously, achiral MNQ adsorbed on the chiral silica became active in CD spectra around its absorption band from 250 ~ 400 nm and showed good mirror relation between the enantiomeric silica pair of D- and L-forms indicating the chiral induction ability of silica to the guest of achiral molecules of MNQ.

**Table S1.** Crystallite size of metallic Ag-loaded into chiral  $\text{SiO}_2$ .

Sample	Crystallite size <sup>[a]</sup> [nm]				
	as-prepared	500 °C	600 °C	700 °C	800 °C
L-form	8.1	12.9	20.0	27.8	36.2
D-form	4.4	9.2	19.9	27.8	42.6

<sup>[a]</sup> Calculated according to the Scherrer equation.

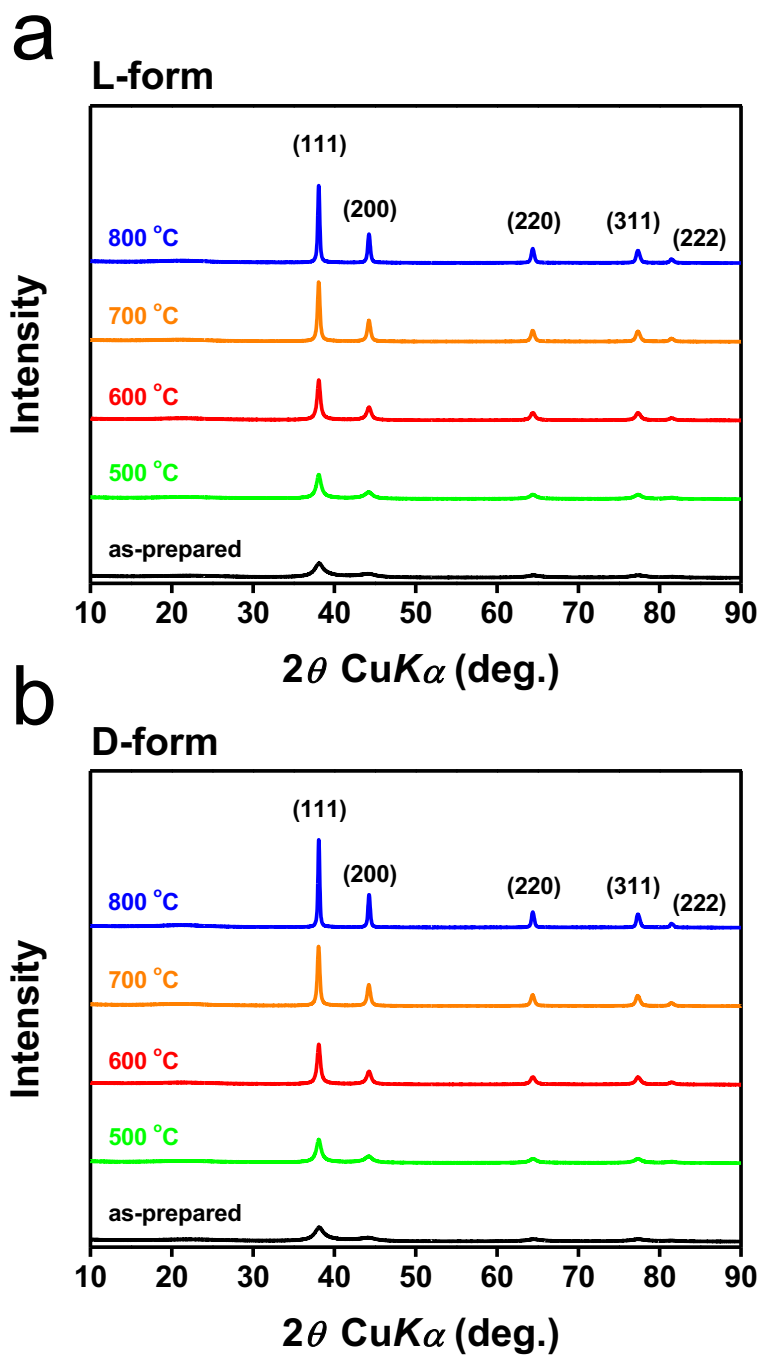


**Fig. S6.** XRD patterns of a) D- and b) L- form of Ag/PEI/Tart@SiO<sub>2</sub> (black line) and those of calcined samples {500 °C (green), 600 °C (red), 700 °C (orange), 800 °C (blue)}.

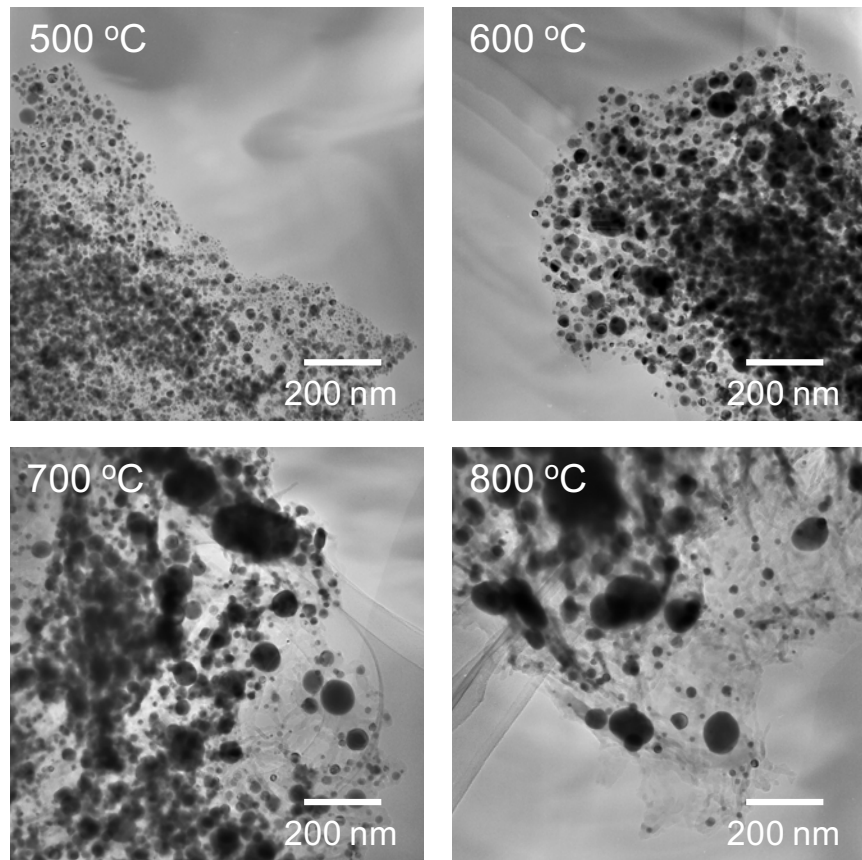


**Fig. S7.** TEM images of L-form  $\text{SiO}_2$ @Ag samples prepared by different calcination temperature at 500, 600, 700 and 800 °C, respectively, ordered from left to right.

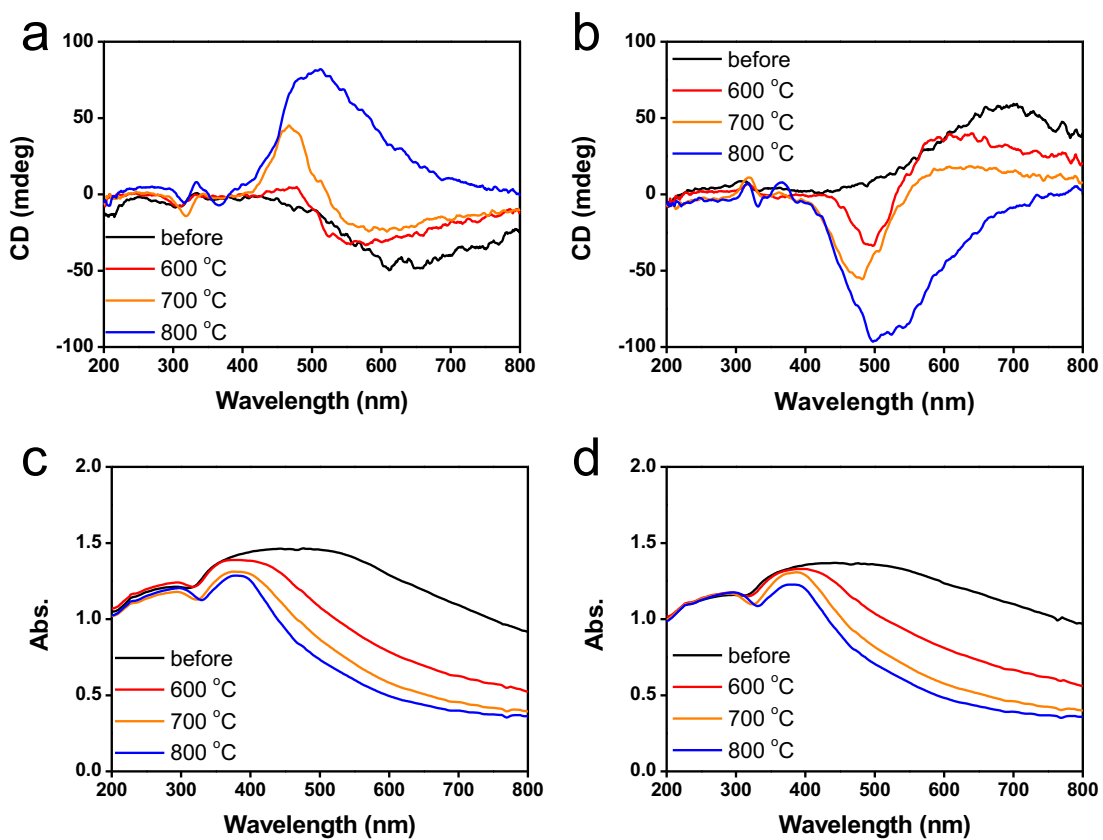


**Fig. S8.** DRCD and UV-Vis spectra of a), c) D- and b), d) L- form of  $\text{Ag/PEI/Tart@SiO}_2$  (black line) and those of calcined samples at 600 °C (red line), 700 °C (orange line) and 800 °C (blue line).

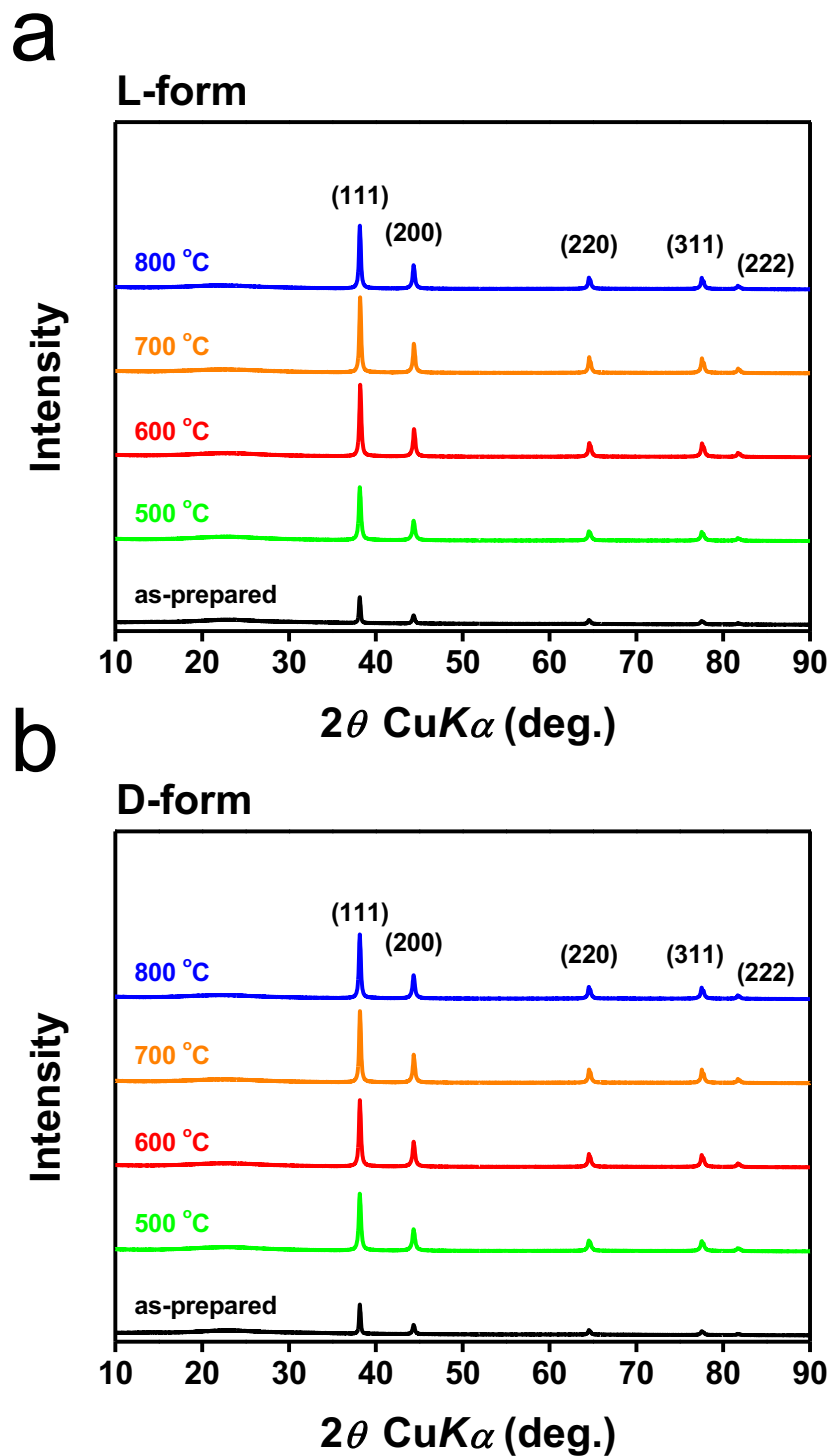


**Fig. S9.** XRD patterns of a) D- and b) L- form of Au/PEI@SiO<sub>2</sub> (black line) and those of calcined samples {500 °C (green), 600 °C (red), 700 °C (orange), 800 °C (blue)}.

**Table S2.** Crystallite size of metallic Au-loaded into chiral SiO<sub>2</sub>.

Sample	Crystallite size <sup>[a]</sup> [nm]				
	as-prepared	500 °C	600 °C	700 °C	800 °C
L-form	47.4	35.6	39.7	44.2	42.2
D-form	34.6	33.5	37.6	43.0	39.3

<sup>[a]</sup> Calculated according to the Scherrer equation.

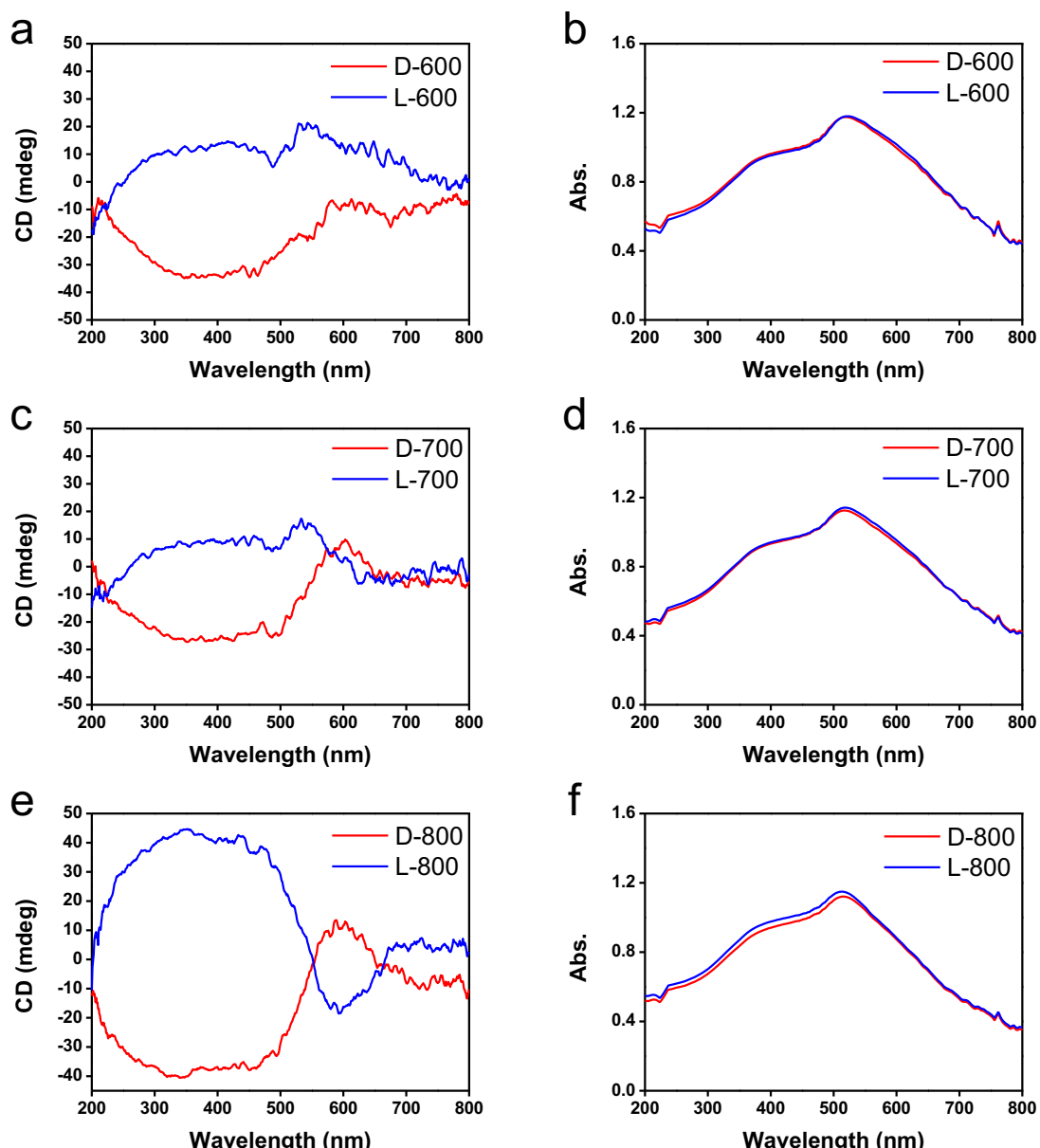


**Fig. S10.** DRCD and UV-Vis spectra of a-b)  $\text{SiO}_2@\text{Au-600}$ , c-d)  $\text{SiO}_2@\text{Au-700}$  and  $\text{SiO}_2@\text{Au-800}$  (red lines for D-form and blue line for L-form).

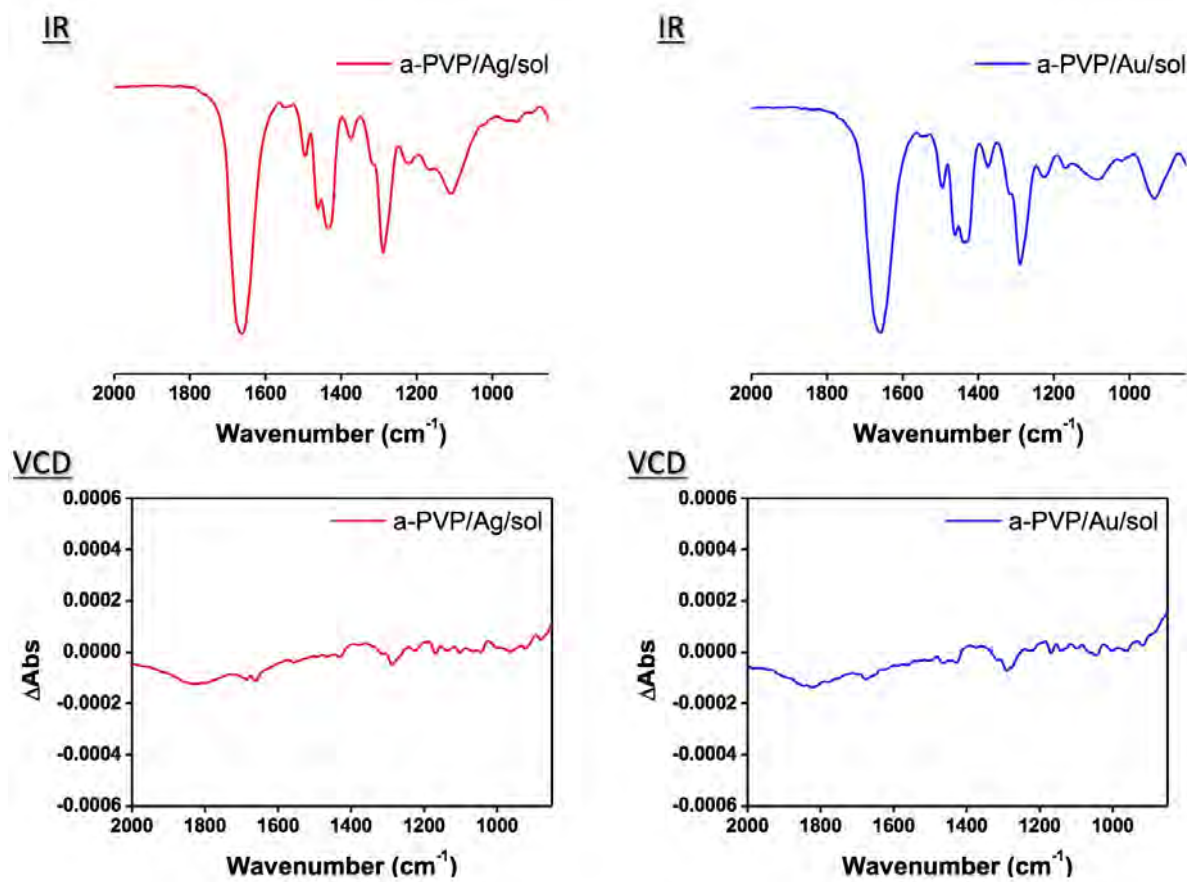


**Fig. S11.** IR and VCD spectra of achiral Au and Ag NPs adsorbed PVP (The achiral Au/sol and achiral Ag/sol were dispersed in 0.25 mL of methanol containing 0.002 g of polyvinylpyrrolidone K90 (PVP). After stirring for several minutes, the solution above was dropped onto the silicon wafer and then subjected to VCD testing. In case of these achiral metallic NPs, no corresponding VCD signals appeared, although there were strong vibration peaks due to C=O in IR spectra.

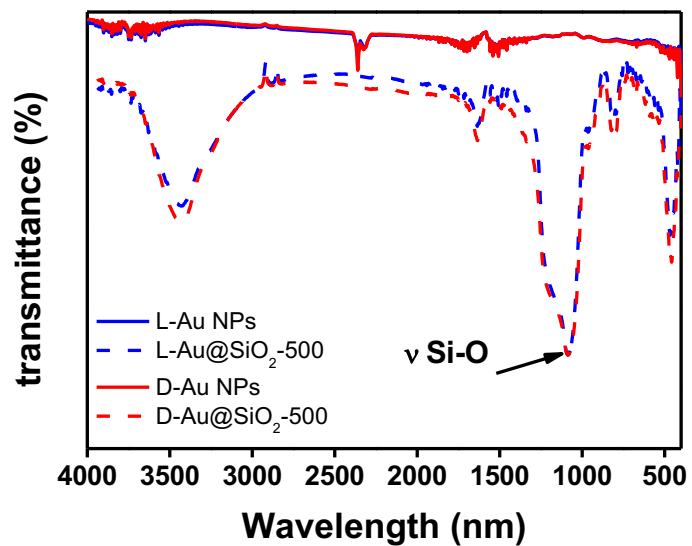


**Fig. S12.** FT-IR spectra of chiral Au@SiO<sub>2</sub>-500 (dash line) and hydrolyzed samples (solid line).

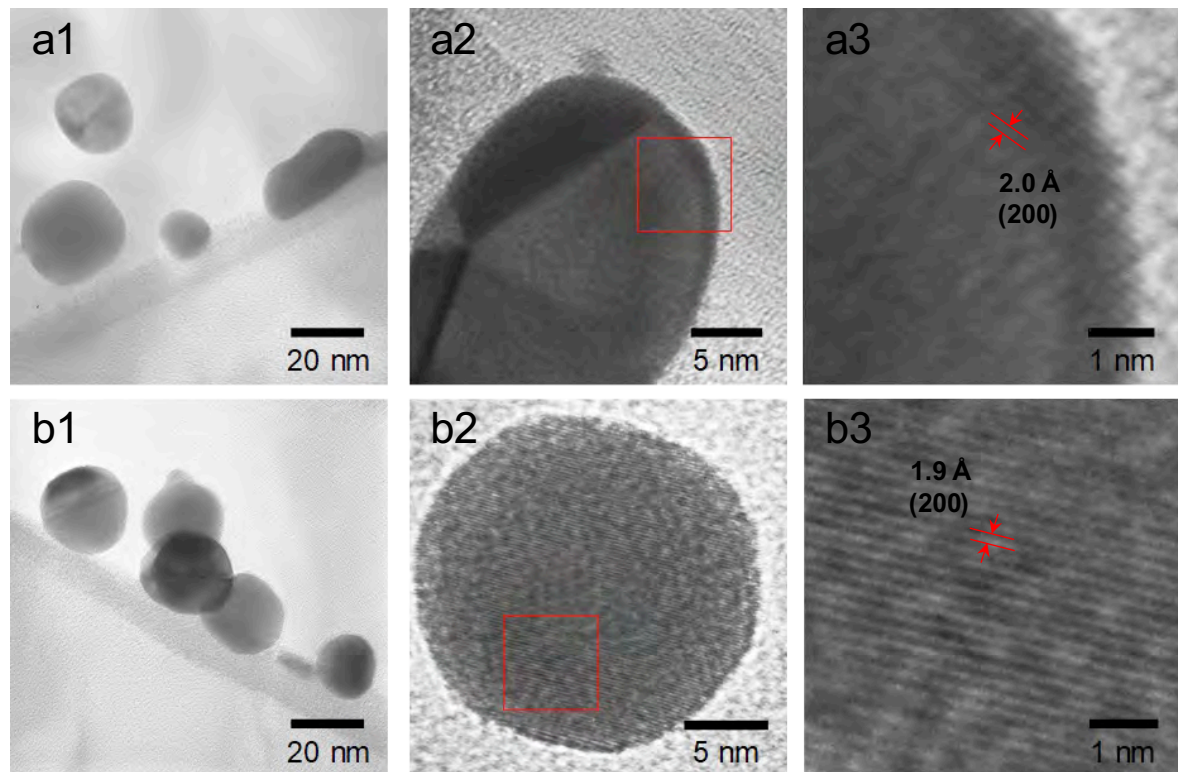


**Fig. S13.** TEM images at various magnifications of NPs for D-Au (a1-a3), L-Au (b1-b3) obtained from hydrolysis of D- and L-Au@SiO<sub>2</sub>-500 by NaOH (aq), respectively.

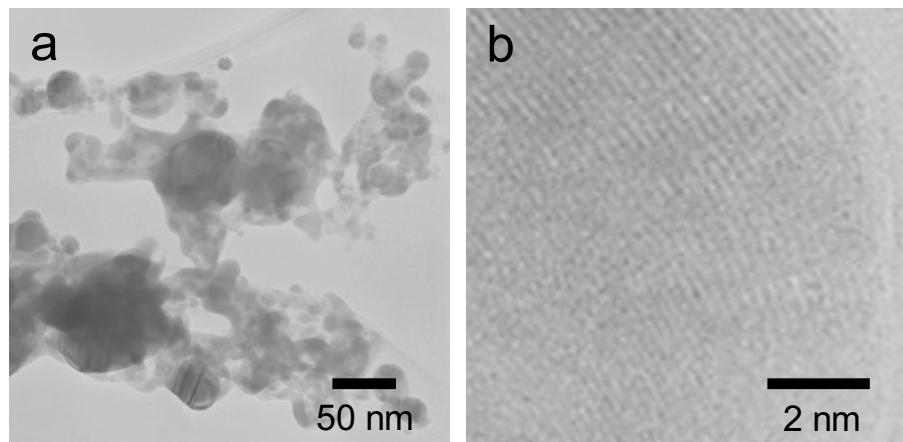


**Fig. S14.** TEM images of a) L-Ag NPs and b) its lattice fringe. The Ag NPs were, obtained by hydrolysis of L-Ag@SiO<sub>2</sub>-600 with NaOH(aq.).

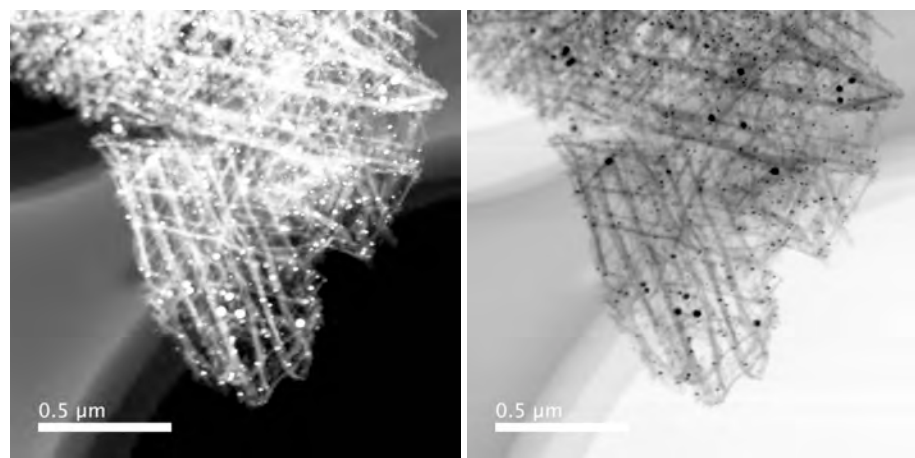


**Fig. S15** TEM images of achiral Au@SiO<sub>2</sub>-500.

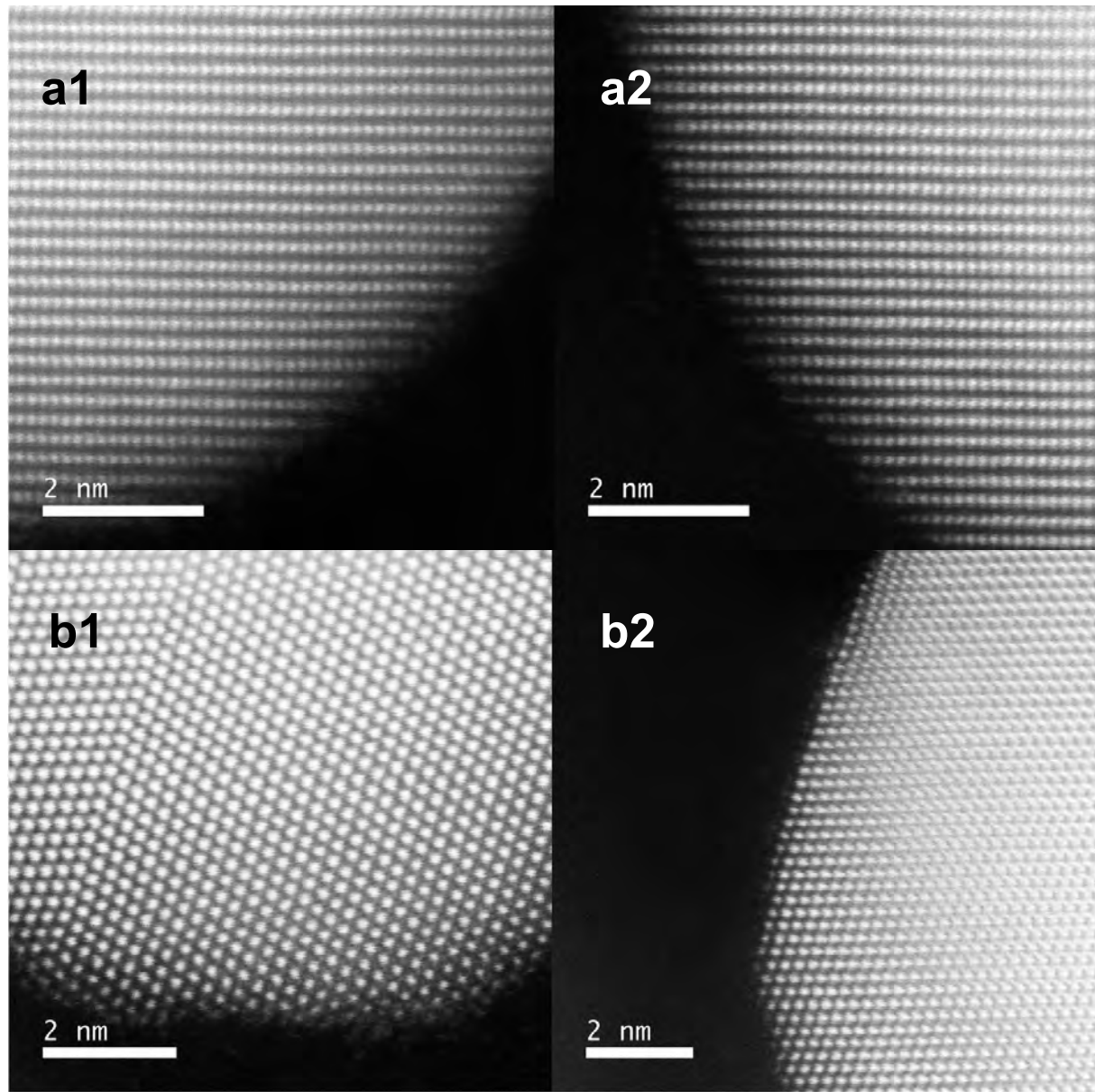


**Fig. S16** Atomic resolution HAADF-STEM images of chiral Au (a1 and a2) and achiral Au (b1 and b2).

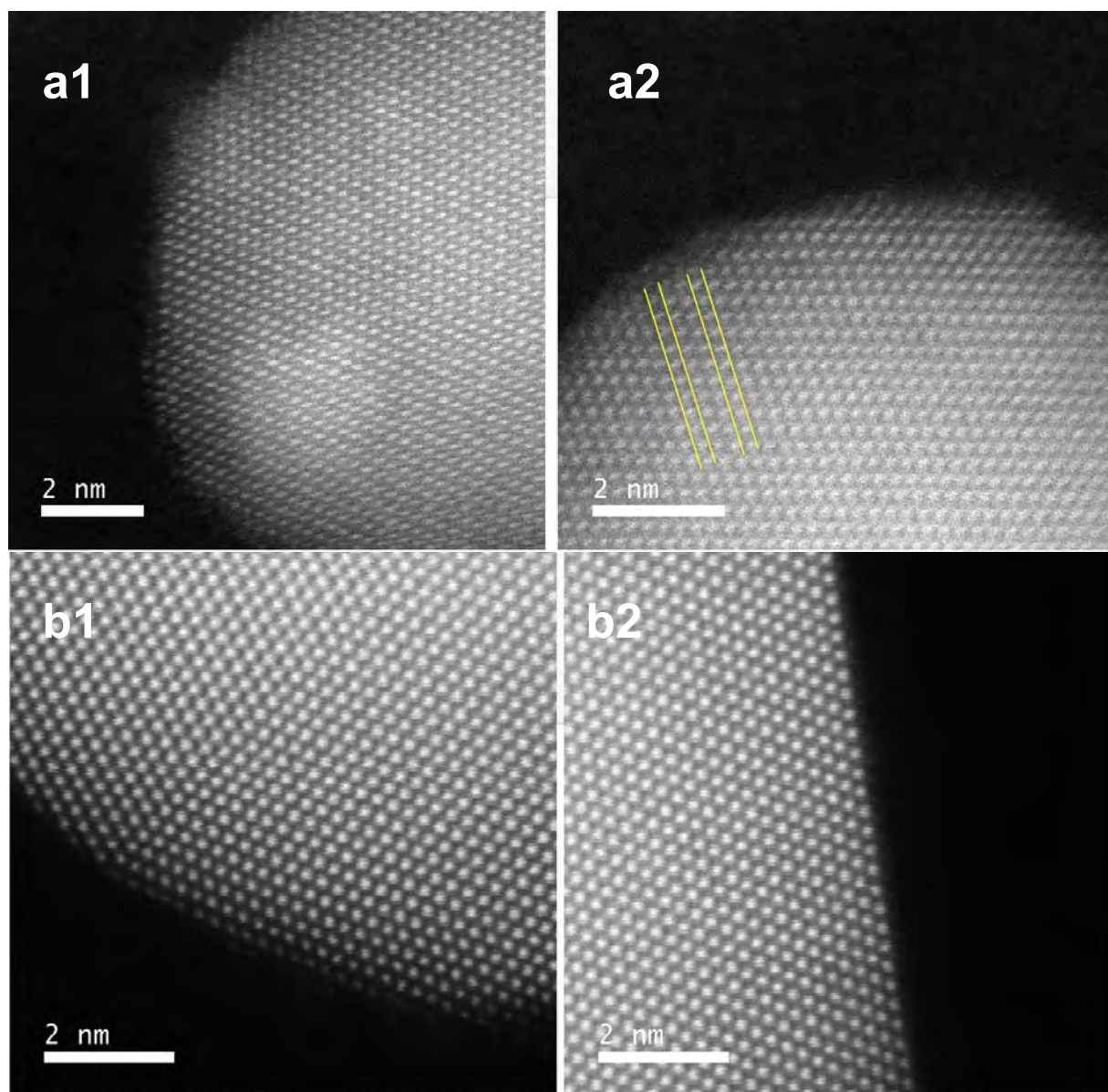


**Fig. S17** Atomic resolution HAADF-STEM images of chiral Ag (a1 and a2) and achiral Ag (b1 and b2).